PHYSICAL REVIEW E **70**, 015501(R) (2004)

# Phase-matching segmented wigglers in free-electron lasers

H. P. Freund
*Science Applications International Corporation, McLean, Virginia 22102, USA*
(Received 6 October 2003; published 30 July 2004)

Since many free-electron lasers use a segmented undulator, it is important to understand the requirements on phase matching between the undulators. A simulation that self-consistently determines the phase slippage between the light and the electrons is used to study these effects, The simulation is found to be in agreement with an analytic formulation of the phase slippage. A seeded x-ray free-electron laser is studied which makes use of a segmented undulator with quadrupoles in the gaps to provide strong focusing. Optimal performance is found for gap lengths corresponding to a phase slippage within about 20% of a wavelength through a unit cell consisting of an undulator and gap.

DOI: 10.1103/PhysRevE.70.015501 PACS number(s): 41.60.Cr

Most current x-ray free-electron laser (FEL) designs are based on self-amplified spontaneous emission (SASE) where shot noise on the beam is amplified in a single pass through a long undulator [1,2]. Because of the need for additional beam focusing and diagnostics in long undulators, these designs use segmented undulators with quadrupole focusing in the gaps. As a result, care is needed in choosing the gap lengths to match the phase slippage of the light relative to the electrons between the undulators. In this paper, the MEDUSA simulation code [3,4] is used to study FEL performance as a function of this gap length for parameters corresponding to the Linac Coherent Light Source (LCLS) at the Stanford Linear Accelerator Center [1].

The phase slippage at the resonant wavelength in a FEL is exactly one wavelength per undulator period; however, this phase slippage varies with wavelength across the gain band. If the undulator lengths in a multiple-segment undulator line are comparable to the exponentiation length but long enough that variation in the slippage is a substantial fraction of a wavelength across the gain band, then coherent amplification at any specific wavelength from undulator-to-undulator is sensitive to the gap length between the undulators. This is precisely the case for the LCLS. In particular, the simulations show that the total phase slippage for each wavelength through the unit cell consisting of an undulator and gap must be close to an integer number of wavelengths for coherent amplification to occur. This hitherto unsuspected effect implies that the detailed shape of the output spectrum will vary with the gap length.

In order to provide physical insight into the results of the numerical simulation, we derive an approximate analytical formula for the phase slippage using a one-dimensional orbit model. It should be emphasized, however, that this model is for insight only, and that MEDUSA implicitly includes the phase slippage in the integration of the particle trajectories in a three-dimensional field model. The fundamental equation is

$$\varphi = -\frac{\omega L}{v_b}\left(1-\frac{v_b}{c}\right), \tag{1}$$

where $\omega$ is the angular frequency, $L$ is the length of the region under consideration, $v_b$ is the axial velocity of the beam, and c is the speed of light *in vacuo*. This formula can be evaluated relatively easily in the gaps between the undulators and in the uniform field regions of the undulators. In the undulator gaps where $v_b/c \cong 1-1/2\gamma_b^2$, where $\gamma_b = 1 + E_b/m_e c^2$, $E_b$ is the beam kinetic energy, and $e$ and $m_e$ are the electronic charge and mass; hence, the phase slippage at the resonance wavelength $\lambda_{\rm res}[=\lambda_w(1+K^2/2)/2\gamma_b^2]$ is

$$\frac{\varphi_{\rm gap}}{2\pi} \cong -\frac{L_{\rm gap}}{\lambda_w(1+K^2/2)}, \tag{2}$$

where $K = eB_w/m_e c^2 k_w$ is the peak undulator strength parameter ($k_w = 2\pi/\lambda_w$). Note that the effects of focusing quadrupoles are neglected in this idealized one-dimensional model, but are included in the MEDUSA simulation. In the uniform undulator region the axial velocity after averaging over the undulator oscillations is $v_b/c \cong 1-(1+K^2/2)/2\gamma_b^2$ and the phase slippage is

$$\frac{\varphi_w}{2\pi} \cong -\frac{L_w}{\lambda_w}\left(1-\frac{\lambda-\lambda_{\rm res}}{\lambda_{\rm res}}\right), \tag{3}$$

at wavelength $\lambda$, where $L_w$, is the length of this region. When $\lambda = \lambda_{\rm res}$ the slippage is one wavelength per wiggler period.

The phase slippage in the entry and exit transitions is more difficult to estimate. The wiggler field in the entry region is $\mathbf{B}_w(z) = B_w \hat{\mathbf{e}}_y \sin^2(\pi z/2N_{\rm trans}\lambda_w)\cos(k_w z)$, where $z$ is measured from the start of the transition region [i.e., $0 \leqslant z \leqslant N_{\rm trans}\lambda_w$]. The exit transition has a symmetric decrease. When $N_{\rm trans} \gg 1$ the velocity changes adiabatically, and the wiggler-averaged orbit approximation can still be used so that

$$\frac{v_b(z)}{c} \cong 1-\frac{1}{2\gamma_b^2}\left[1+\frac{K^2}{2}\sin^4\left(\frac{\pi}{2}\frac{z}{N_{\rm trans}\lambda_w}\right)\right]. \tag{4}$$

The sum of the phase slippages in the entrance and exit regions at the resonant wavelength, therefore, is

$$\frac{\varphi_{\rm trans}}{2\pi} = \frac{2\omega N_{\rm trans}\lambda_w}{c} - 2\omega\int_0^{N_{\rm trans}\lambda_w}\frac{dz'}{v_b(z')} \cong -\frac{2L_{\rm eff}}{\lambda_w(1+K^2/2)}, \tag{5}$$

where $L_{\rm eff} = N_{\rm trans}\lambda_w(1+3K^2/16)$.

 ©2004 The American Physical Society

As a consequence, the total phase advance through an undulator and gap is

$$\frac{\varphi_{\rm tot}}{2\pi} \cong -\frac{L_{\rm gap}+2L_{\rm eff}}{\lambda_w(1+K^2/2)} - \frac{L_w}{\lambda_w}\left(1-\frac{\lambda-\lambda_{\rm res}}{\lambda_{\rm res}}\right). \qquad (6)$$

The variation in $\varphi_{\rm tot}$ with $\lambda$ in the gaps and the transition regions is small and may be neglected. However, this is not necessarily so in the uniform undulator regions. The amplification band in a typical FEL is small; hence, $|\lambda-\lambda_{\rm res}| \ll \lambda$. However when $L_w \gg \lambda_w$, the phase shift in the uniform undulator sections can vary by an appreciable fraction of a wavelength across the FEL amplification band, and this is found in simulation.

Once again, we note that Eq. (6) is derived under highly idealized assumptions and is meant only to provide physical insight into the variation in phase slippage with wavelength. In particular, $N_{\rm trans}=1$ in the case under study, and the estimate of $\varphi_{\rm trans}$ (5) based upon the adiabatic orbit approximation breaks down. Nevertheless, it is found that Eq. (6) is in reasonable agreement with MEDUSA, which does not employ the wiggler-averaged orbit formulation and is not so limited.

MEDUSA [1,2] is a three-dimensional (3D), polychromatic simulation code that models either planar or helical wiggler geometry and treats the electromagnetic field as a superposition of Gaussian modes. The field equations are integrated simultaneously with the 3D Lorentz force equations for an ensemble of electrons. No wiggler-average orbit approximation is used, and MEDUSA can propagate the electron beam through a complex undulator/transport line including multiple undulator sections, quadrupole and dipole corrector magnets, focusing/defocusing (FODO) lattices, and magnetic chicanes. In particular, the phase slippage between the light and each electron is integrated self-consistently throughout the simulation.

A simplified configuration for the LCLS [1] is used for this paper. The electron beam is Gaussian with a 14.36 GeV energy and a 3272 A peak current. The beam is not symmetric, and the normalized emittances are 0.8869 and 0.8198 mm mrad in the $x$ and $y$ directions, respectively. The beam is elliptical with rms beam dimensions of 19.32 (24.22) $\mu$m in the $x$ ($y$) direction and 24.22 $\mu$m. Since many simulation runs are required to fully examine the phase slippage, the beam model is simplified by assuming that the energy spread vanishes. This results in a shorter gain length and a larger gain bandwidth than is anticipated in the LCLS, but does not change any of the essential conclusions regarding the phase slippage while reducing the computational load significantly.

The undulator line consists of 33 undulators with quadrupoles located in the centers of the gaps. The undulators have a peak on-axis field ($B_w$) of 13.25 kG and a period ($\lambda_w$) of 3.0 cm. An analytic field model of a flat-pole-face undulator field is used with a uniform field section of 112 periods in length and one-period entry and exit transitions. The field is oriented so that the wiggle motion is in the $x$ direction. A transition region of one period in length is used ($N_{\rm trans}=1$). The quadrupoles are configured as a FODO lattice. A hard-edged field model is used with a field gradient of

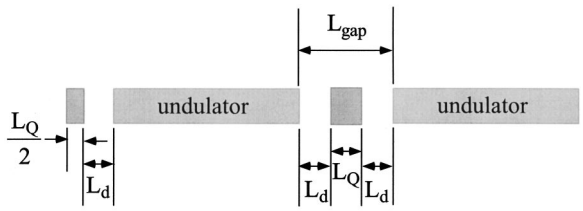


FIG. 1. Schematic illustration of the first two quadrupoles and undulators.

10.6 kG/cm over a length of 0.05 m. The Twiss $\alpha$ parameters are assumed to be zero, so we configure the undulator line with a half-quadrupole before the first undulator to rotate the phase space. This is illustrated schematically in Fig. 1 for the first two undulators and quadrupoles. Here $L_Q$ is the length of the quadrupole, $L_d$ is the length of the drift region separating the undulators and quadrupoles, and the total gap length is $L_{\rm gap}=L_Q+2L_d$.

The simulations correspond to a seeded amplifier at fixed wavelengths. An example of the results is shown in Fig. 2 where the power is plotted versus distance for a gap length of 0.27 m at a wavelength of 1.500 Å with an initial drive power of about 500 W corresponding to the noise power. After the initial transient region, the power grows exponentially until shortly before saturation at about 91 m with a power of 21.5 GW. Note that the undulator/FODO line in the LCLS is longer than required to reach saturation even using the anticipated beam energy spread. The evolution of the transverse beam dimensions versus distance for this case is shown in Fig. 3. Observe that the FODO lattice initially focuses the beam in the $x$ direction and defocuses in the $y$ direction.

The phase slippage in simulation differs from the analytic formula because there is an axial velocity spread corresponding to the emittance. Nevertheless, comparison between simulation and the analytic formula is good. For example, the phase slippage in the transition regions is about 0.91$\lambda$ using Eq. (5). This compares well with the average phase slippage of 0.92$\lambda$ for all of the electrons in simulation. The phase slippage across the unit cell consisting of the undulator and gap is about 114$\lambda$ for a gap length of 0.27 m at the

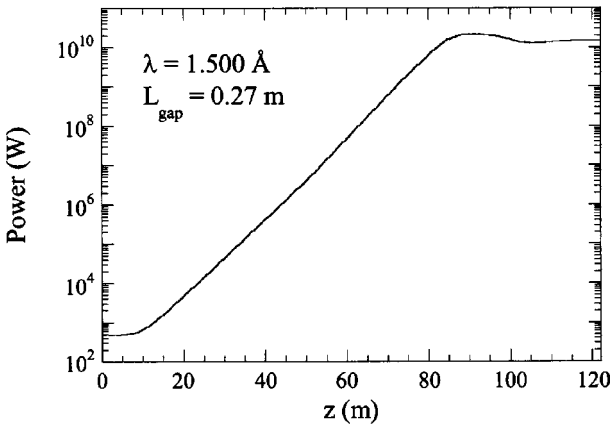


FIG. 2. Evolution of the power vs distance for a wavelength of 1.50 Å and a gap length of 0.27 m.

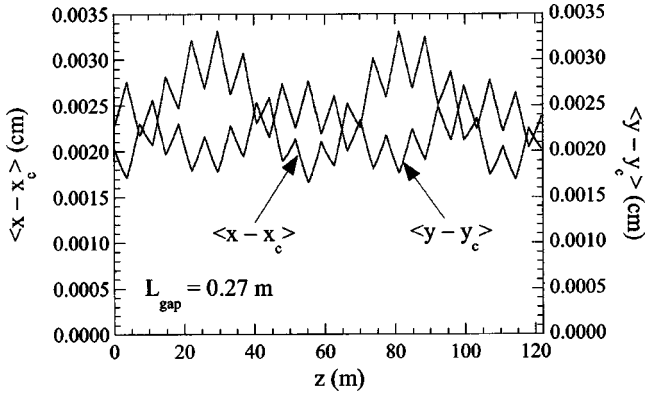


FIG. 3. Evolution of the transverse dimensions of the beam as functions of distance.

resonant wavelength of 1.4975 Å. At the wavelength of 1.500 Å used in Fig. 2, this phase slippage is 113.86λ. The full width of the amplification band found in simulation extends from about 1.490 to 1.506 Å, but this bandwidth would be smaller had an energy spread been used in simulation. Since $\Delta\lambda/\lambda_{res} \approx \pm 0.008$ and the uniform undulator region is $112\lambda_w$ long, the phase slippage in the undulator will vary by as much as ±80% of a wavelength across the amplification band. However, coherent amplification does not occur over the entire amplification band at this, or any other, choice of gap length.

The variation in performance with gap length is shown in Fig. 4, where the output power at the end of the undulator line (circles) and phase slippage (as found in MEDUSA) through a unit cell (squares) is plotted versus gap length. Note that no effort to retune the FODO lattice has been made as the gap length changes. Since the undulator line is longer than required to reach saturation, the points shown in the figure correspond to a range of cases from where the power has saturated prior to the end of the undulator line to cases where there is no saturation at all. The phase slippage increases linearly with gap length, and it is clear that the FEL will reach saturation when the phase slippage through the unit cell is close to an integer number of wavelengths, but this can vary by as much as about ±0.2λ without seriously

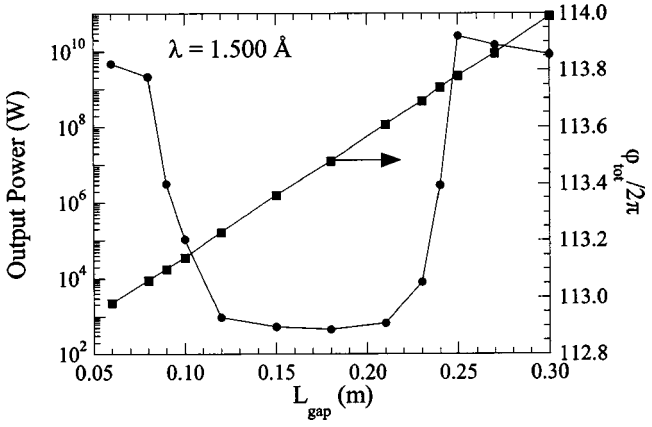


FIG. 4. Variation in the output power (circles) and phase slippage through a unit cell (squares) with gap length.

degrading performance. The sharp rise and fall in the power is due to the fact that there is no coherent amplification from undulator-to-undulator when the phase mismatch is outside of this range. Since this is smaller than the total variation in phase slippage with wavelength across the amplification band in the undulators ($\approx \pm 0.8\lambda$), the phase mismatch associated with the segmented undulator will result in a narrowing of the spectrum. Note also that the phase slippage varies by an integer number of wavelengths as the gap length increases by $\lambda_w(1+K^2/2) \approx 0.24$ m for the LCLS.

It should be remarked that if there were high gain in each undulator, then the system would not be sensitive to the gap length [5]. For undulators much longer than an e-folding length, the phases of the electrons self-adjust over a distance comparable to an e-folding length after which exponential growth resumes. However, the undulators for most SASE x-ray FEL designs are comparable to the e-folding length. For the LCLS case, the e-folding length is approximately 3.3 m [6], and is comparable to the undulator length of 3.42 m. As a result, the undulators are not long enough to overcome the initial transient response due to a mismatch in the phase slippage, and care is needed to ensure that the phase slippage is properly matched for coherent amplification in each undulator.

As noted above, the phase slippage in the uniform undulator region can vary by a substantial fraction of a wavelength over the amplification band. This implies that the proper phase match for coherent amplification over the undulator/FODO line will occur at different wavelengths as the gap length changes. The change in gap length required to maintain a constant phase slippage as the wavelength changes is

$$\Delta L_{\mathrm{gap}} \approx L_w \frac{\Delta\lambda}{\lambda_{\mathrm{res}}}(1 + K^2/2), \tag{7}$$

so that $\Delta L_{\mathrm{gap}}$ varies across the amplification band by about 0.27 m for the LCLS parameters. Because $\Delta L_{\mathrm{gap}} > \lambda_w(1 + K^2/2)$, a range of wavelengths in the amplification band can be found that reaches saturation for any desired gap length. This is summarized in Fig. 5 where the range of wavelengths that reach saturation is plotted versus gap length. The "error bars" in the figure represent the range of wavelengths over which saturation is reached and the central circle corresponds to the wavelength with a slippage that is an integer number of wavelengths. The vertical dashed lines mark a change in gap length of 0.24 m.

There are several characteristics shown in Fig. 5 that deserve mention. First, the range of wavelengths that reach saturation increases linearly with gap length in accord with Eq. (7). Second, the expected periodicity at 0.24 m is found in simulation. Third, while the full amplification band extends over 1.490−1.506 Å, the requirement that the phase slippage must be close to an integer number of wavelengths through a unit cell results in a narrowing of this band and, in some cases, two distinct amplification bands are found that are subsets of the full amplification band.

To summarize, the effects of phase slippage between the light and the electrons in a segmented-undulator FEL have

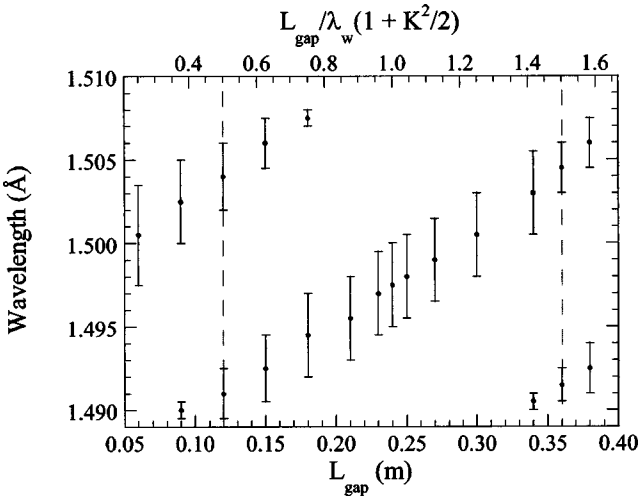


FIG. 5. Variation in the range of wavelengths that reach saturation vs gap length.

been studied using MEDUSA which self-consistently integrates this phase slippage. The specific case studied corresponds to a seeded x-ray EEL with parameters corresponding to the LCLS except that the beam energy spread has been neglected to ease the computational load. This simplification results in a larger growth rate and a wider amplification band, but does not alter any of the conclusions concerning the effects of the phase slippage. The phase slippage observed in MEDUSA is in agreement with an analytic model for this slippage. It is found that the phase slippage through a unit cell consisting of an undulator and gap must be within about 20% of a wavelength for optimal performance for the parameters studied. Since the variation in phase slippage through the undulators with wavelength across the amplification band exceeds this value, there is a narrowing of the amplification spectrum. This means that (1) saturation can be expected in the LCLS for any choice of gap length, and (2) it may be possible to tune a seeded FEL using both energy and gap length.

These conclusions were obtained for a seeded FEL with parameters consistent with the LCLS design, and may differ quantitatively for alternate choices of the parameters. Further, this analysis was conducted for a seeded EEL amplifier, and the implications for SASE FELs may be more complex. In a SASE FEL, the noise power at each frequency is independently amplified in the exponential regime prior to saturation. In this regime, the conclusions, such as the frequency band(s) that can be coherently amplified, will be similar to those for a seeded amplifier. However, when a SASE FEL nears saturation, there is strong competition between the different frequency components that results in a substantial spectral narrowing. While the effects of this mode of competition are not included in the present analysis, it is possible that the gap lengths can be adjusted for detailed spectral control or to reduce spiking modes.

This work was supported by the JTO. The author would like to acknowledge helpful discussions with G. Dattoli, B. Faatz, L. Gianessi, Z. Huang, S.V. Milton, H.-D. Nuhn, P.G. O'Shea, and S. Reiche.

[1] LCLS Design Group, LCLS Design Report, NTIS Doc. No. DE98059292, 1998 (copies may be ordered from the National Technical Information Service, Springfield, VA 22162).

[2] J. Rossbach, Nucl. Instrum. Methods Phys. Res. A **375**, 269 (1996).

[3] H. P. Freund and T. M. Antonsen Jr., *Principles of Free-Electron Lasers*, 2nd ed. (Chapman & Hall, London, 1996).

[4] H. P. Freund, S. G. Biedron, and S. V. Milton, IEEE J. Quantum Electron. **36**, 275 (2000).

[5] N. A. Vinokurov, Nucl. Instrum. Methods Phys. Res. A **375**, 264 (1996).

[6] M. Xie, Proc. IEEE 1995 Particle Accelerator Conference, Vol. 183, IEEE Cat. No. 95CH35843, 1995.